Sliding Mode Current Control with Luenberger Observer applied to a Three Phase Induction Motor

1st Enrique Paiva
Universidad del Cono Sur de las Américas (UCSA)
Asunción, Paraguay
enpaiva93@gmail.com

2nd Larizza Delorme
Universidad del Cono Sur de las Américas (UCSA)
Asunción, Paraguay
laridelorme@gmail.com

3rd Marcos Gomez-Redondo
Universidad del Cono Sur de las Américas (UCSA)
Asunción, Paraguay
gomezredondomarcos@gmail.com

4th Esteban Cristaldo
Universidad del Cono Sur de las Américas (UCSA)
Asunción, Paraguay
e.cristaldo27@gmail.com

5th Jorge Rodas
Universidad Nacional de Asunción
Luque, Paraguay
jrodas@ing.una.py

6th Yassine Kali
École de Technologie Superiéure
Montreal, Canada
y.kali88@gmail.com

7th Raul Gregor
Universidad Nacional de Asunción
Luque, Paraguay
rgregor@ing.una.py

***Abstract*—In this paper, the problem of controlling three-phase induction motors with unmeasurable states is tackled. To that end, a finite-time robust nonlinear current control is applied. The controller employed is the first order sliding mode with exponential reaching law variant. Moreover, in order to estimate some variables that are not measurable, such as the rotor current, a state observer based on Luenberger observer is implemented. Simulation results show a good tracking of the desired reference, given that there exist some dynamics which were not modeled and there are fast changes in the reference.**

***Index Terms*—Current control, induction motor drives, sliding mode control.**

NOMENCLATURE

ERL	Exponential reaching law.
IM	Induction motor.
PI	Proportional-integral.
SMC	Sliding mode control.
VSI	Voltage source inverter.

I. INTRODUCTION

Induction Motors (IMs) have been widely applied in industrial applications due to its merits of low cost, simple and robust construction and ease of maintenance [1]. Currently, the focus of the study of new control techniques is oriented towards multi-phase IMs with more than three phases, which are gaining terrain in high power applications [2]–[6]. However, in low to medium power requirement applications, three-phase IMs keep its validity, being the preferred choice of the industrial complex for the mechanical propulsion of the machinery of the various processes. Although there is over a century of experience with three-phase IMs, developing precise control systems is still a challenge, considering that these machines are modeled as multi-variable systems and not all variables are available for measurement, in addition of having the aggravating factor of being related non-linearly to each other which leads to inaccuracies in the estimations and control of variables when classic control methods are applied to simplified and linear models of IMs [7]–[9].

The traditional method for controlling a three-phase machine is the field-oriented control with Proportional-Integral (PI) controller [10]. For the mitigation of harmonic currents, one PI and multiple resonant controllers can be implemented in just one rotating frame at the fundamental frequency, so as to reduce the computation required when using multiple synchronous frames [11]. Other popular techniques are the direct torque control and the current control using the model predictive control, in which the main advantage is that no modulator is needed [12], [13]. Among various control methods of IMs, sliding mode control (SMC) is gaining more and more attention in both academic and industrial communities [14], [15]. Compared to the conventional vector control using linear controller plus modulation, SMC is a fast and robust alternative for nonlinear systems, when the response with the traditional PI has not enough quality [16].

Within the range of control algorithms related to the sliding mode, the Exponential Reaching Law (ERL) [17], [18] provides an adaptation of the gains depending on the sliding surface, this allows to reduce the chattering phenomenon during the sliding phase and with the appropriate parameters the convergence can be increased during the reach phase. These characteristics are suitable to implement in three-phase induction motors. Therefore, it is proposed to simulate this algorithm for the current control of these motors. In general, the speed or the torque is controlled in an outer loop and the current controller in the inner loop can be replaced in order to get a better response [19]. This work aims to improve the current control of the inner loop, so only the current control is considered.

The present paper is divided into five sections as follows. In the following section, the full mathematical models of the three-phase induction motor and the rearranging of these equations for the sliding mode controller mathematical structure are presented. In Section III, the sliding mode controller with ERL is developed. In Section IV, numerical simulations of IM studied to show the performance of the proposed controller. The conclusion is in the last section.

II. Mathematical Model

The dynamical model of the IM depicted in Fig. 1 is modeled as an electromechanical system that transforms electrical energy into mechanical defined by a set of differential equations. In order to reduce the complexity and apply control techniques over the machine, the equations are presented in stationary reference frame.

A. IM model in stationary reference frame ($\alpha - \beta$)

The IM model considering a stationary reference frame $\alpha - \beta$ for describe the dynamic of the machine, is given by:

$$\begin{aligned} v_{\alpha s} &= R_s i_{\alpha s} + \dot{\lambda}_{\alpha s} \\ v_{\beta s} &= R_s i_{\beta s} + \dot{\lambda}_{\beta s} \\ \lambda_{\alpha s} &= L_s i_{\alpha s} + L_m i_{\alpha r} \\ \lambda_{\beta s} &= L_s i_{\beta s} + L_m i_{\beta r} \\ v_{\alpha r} &= 0 = R_r i_{\alpha r} + \dot{\lambda}_{\alpha r} + w_r \lambda_{\beta r} \\ v_{\beta r} &= 0 = R_r i_{\beta r} + \dot{\lambda}_{\beta r} - w_r \lambda_{\alpha r} \\ \lambda_{\alpha r} &= L_r i_{\alpha r} + L_m i_{\alpha s} \\ \lambda_{\beta r} &= L_r i_{\beta r} + L_m i_{\beta s} \end{aligned} \tag{1}$$

where L_s, L_r, L_{ls}, L_{lr} and L_m are the stator and rotor inductance, estator and rotor leakage inductance and the magnetization inductance respectively. The resistances for estator and rotor are R_s and R_r. Voltages, currents and flux in $\alpha - \beta$ plane are represented by v, i and λ respectively. The electromagnetic torque T_e is given in terms of the rotor and stator current as:

$$T_e = \frac{3}{2} P L_m \left(i_{\beta s}\, i_{\alpha r} - i_{\alpha s}\, i_{\beta r} \right), \tag{2}$$

being P the pole pairs of the IM. The relationship between the electrical variables of the machine and the load T_L in terms of the rotor speed, is given by:

$$J\, \dot{w}_r = -B w_r + P \left(T_e - T_L \right), \tag{3}$$

where J represents the moment of inertia while B is the friction coefficient. The rotor speed w_r which is related to the mechanical speed by the number of pole pairs by:

$$w_r = w_m P. \tag{4}$$

B. IM model in state variables

The model of the IM in state variables is obtained from (1)-(3), and is represented by:

$$\dot{\mathbf{x}}(t) = \mathbf{f}(\mathbf{x}, t) + \mathbf{g}\, \mathbf{u}(t) \tag{5}$$

where $\mathbf{x}(t) \in \mathbb{R}^5$ is a five-dimensional vector of state variables and $\mathbf{u}(t) \in \mathbb{R}^2$ is a two-dimensional vector of inputs.

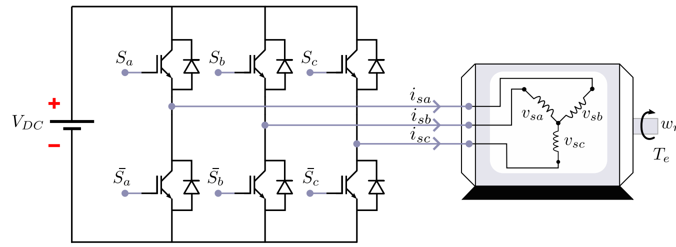

Fig. 1. 3-phase 2-level VSI scheme connected to a IM.

By considering flux equations, their derivatives are represented by:

$$\begin{bmatrix} \dot{\lambda}_{\alpha s} \\ \dot{\lambda}_{\beta s} \\ \dot{\lambda}_{\alpha r} \\ \dot{\lambda}_{\beta r} \\ \dot{w}_r \end{bmatrix} = \begin{bmatrix} L_s & 0 & L_m & 0 & 0 \\ 0 & L_s & 0 & L_m & 0 \\ L_m & 0 & L_r & 0 & 0 \\ 0 & L_m & 0 & L_r & 0 \\ 0 & 0 & 0 & 0 & 1 \end{bmatrix} \begin{bmatrix} \dot{i}_{\alpha s} \\ \dot{i}_{\beta s} \\ \dot{i}_{\alpha r} \\ \dot{i}_{\beta r} \\ \dot{w}_r \end{bmatrix} \tag{6}$$

with:

$$\begin{aligned} \dot{\lambda}_{\alpha s} &= -R_s i_{\alpha s} + v_{\alpha s} \\ \dot{\lambda}_{\beta s} &= -R_s i_{\beta s} + v_{\beta s} \\ \dot{\lambda}_{\alpha r} &= -R_r i_{\alpha r} - w_r \left(L_m\, i_{\beta s} + L_r\, i_{\beta r} \right) \\ \dot{\lambda}_{\beta r} &= -R_r i_{\beta r} - w_r \left(L_m\, i_{\alpha s} + L_r\, i_{\alpha r} \right) \\ \dot{w}_r &= -\frac{B}{J}\, w_r + \frac{3}{2} P^2 \frac{L_m}{J} \left(i_{\beta s}\, i_{\alpha r} - i_{\alpha s}\, i_{\beta r} \right) - \frac{P}{J}\, T_L \end{aligned} \tag{7}$$

Then, by rearranging (6) and (7) the following equivalences are given:

$$\mathbf{x}(t) = \begin{bmatrix} i_{\alpha s} & i_{\beta s} & i_{\alpha r} & i_{\beta r} & w_r \end{bmatrix}$$

$$\mathbf{L} = \begin{bmatrix} L_s & 0 & L_m & 0 & 0 \\ 0 & L_s & 0 & L_m & 0 \\ L_m & 0 & L_r & 0 & 0 \\ 0 & L_m & 0 & L_r & 0 \\ 0 & 0 & 0 & 0 & 1 \end{bmatrix}$$

$$\mathbf{f}(\mathbf{x}, t) = \mathbf{L}^{-1} \begin{bmatrix} -R_s\, i_{\alpha s} \\ -R_s\, i_{\beta s} \\ -R_r\, i_{\alpha r} - w_r \left(L_m\, i_{\beta s} + L_r\, i_{\beta r} \right) \\ -R_r\, i_{\beta r} + w_r \left(L_m\, i_{\alpha s} + L_r\, i_{\alpha r} \right) \\ \frac{3}{2} \frac{P^2}{J} L_m \left(i_{\beta s}\, i_{\alpha r} - i_{\alpha s}\, i_{\beta r} \right) .. \\ \qquad .. - \frac{B}{J}\, w_r - \frac{P}{J}\, T_L \end{bmatrix}$$

$$\mathbf{g} = \mathbf{L}^{-1} \begin{bmatrix} 1 & 0 \\ 0 & 1 \\ 0 & 0 \\ 0 & 0 \\ 0 & 0 \end{bmatrix} \qquad \mathbf{u}(t) = \begin{bmatrix} v_{\alpha s}, v_{\beta s} \end{bmatrix}^T$$

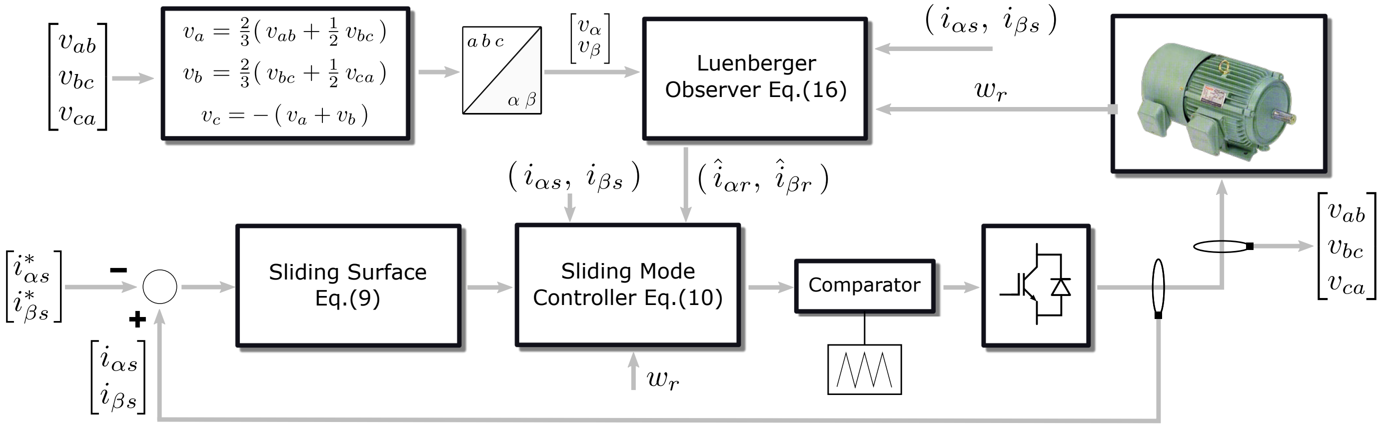

Fig. 2. Block diagram of the closed-loop IM.

III. Proposed SMC-based Current Regulator

The proposed controller (Fig. 2) consists of a first-order SMC with ERL that will force the output vector $\chi = \mathbf{C}\,\mathbf{x}(t) = [\,i_{\alpha s},\ i_{\beta s}\,]^T$ to converge to the desired reference currents $\chi^* = [\,i^*_{\alpha s},\ i^*_{\beta s}\,]^T$. For this purpose, the matrix $\mathbf{C}$ is:

$$\mathbf{C} = \begin{bmatrix} 1 & 0 & 0 & 0 & 0 \\ 0 & 1 & 0 & 0 & 0 \end{bmatrix} \tag{8}$$

Hence, the sliding surface selected here is a PI surface that has the following expression:

$$\mathrm{S} = (\chi - \chi^*) + K_i \int_0^t (\chi - \chi^*)\, dt. \tag{9}$$

where K_i is a positive constant. Otherwise, the SMC with ERL is described by the following equation:

$$\dot{\mathrm{S}} = -\mathrm{K}_1\,\mathrm{S} - \mathrm{K}_2(\mathrm{S})\,\mathrm{sign}(\mathrm{S}) \tag{10}$$

where K_1 is a definite positive diagonal matrix and $\mathrm{K}_2(\mathrm{S})$ is defined by:

$$\mathrm{K}_2(\mathrm{S}) = \begin{bmatrix} \dfrac{k_{21}}{N(\mathrm{S}_1)} & 0 \\ 0 & \dfrac{k_{22}}{N(\mathrm{S}_2)} \end{bmatrix} \tag{11}$$

where $N(\mathrm{S}_i) = \delta_0 + (1-\delta_0)\,\mathrm{e}^{-a\,|\mathrm{S}_i|^p}$ for $i = 1, 2$ with $0 < \delta_0 < 1$ and $a, p > 0$ [18]. The constants k_{21} and k_{22} are positive constants and $\mathrm{sign}(\mathrm{S}) = [\mathrm{sign}(\mathrm{S}_1),\ \mathrm{sign}(\mathrm{S}_2)]^T$ is the signum vector with:

$$\mathrm{sign}(\mathrm{S}_i) = \begin{cases} 1, & \text{if } \mathrm{S}_i > 0, \\ 0, & \text{if } \mathrm{S}_i = 0, \quad \text{for } i = 1, 2 \\ -1, & \text{if } \mathrm{S}_i < 0. \end{cases} \tag{12}$$

The law control equation is obtained by applying the first derivative of (9) and adding the equations (5) - (10):

$$\dot{\mathrm{S}} = (\dot{\chi} - \dot{\chi}^*) + K_i\,(\chi - \chi^*) \tag{13}$$

$$-\mathrm{K}_1\,\mathrm{S} - \mathrm{K}_2(\mathrm{S})\,\mathrm{sign}(\mathrm{S}) = (\dot{\chi} - \dot{\chi}^*) + K_i\,(\chi - \chi^*) \tag{14}$$

$$\begin{aligned} -\mathrm{K}_1\,\mathrm{S} - \mathrm{K}_2(\mathrm{S})\,\mathrm{sign}(\mathrm{S}) &= \mathbf{C}\,\mathbf{f}(\mathbf{x}, t) + \mathbf{C}\,\mathbf{g}\,\mathbf{u}(t).. \\ &.. \ - \dot{\chi}^* + K_i\,(\chi - \chi^*) \end{aligned} \tag{15}$$

Isolate the variable $\mathbf{u}(t)$ of the expression (15) gives the following control law:

$$\begin{aligned} \mathbf{u}(t) = (\mathbf{C}\,\mathbf{g})^{-1}\,(-\mathrm{K}_1\,\mathrm{S} - \mathrm{K}_2(\mathrm{S})\,\mathrm{sign}(\mathrm{S}) - \mathbf{C}\,\mathbf{f}(\mathbf{x}, t) \ .. \\ .. \ + \dot{\chi}^* - K_i\,(\chi - \chi^*)) \end{aligned} \tag{16}$$

The stability analysis of the closed-loop system can be found in [20].

A. Luenberger-Based Rotor Current Estimation

Since the rotor currents in the three-phase induction motor cannot be measured in practice, an estimator based on the Luenberger observer is used [21]–[23]. The equations of this observer are shown in the following expression:

$$\begin{aligned} \dot{\hat{\zeta}} &= \mathcal{A}(w_r)\,\hat{\zeta} + \mathcal{B}\,\mathrm{U} + \mathrm{L}\,(\chi - \mathcal{C}\,\hat{\zeta}) \\ \mathcal{Y} &= \mathcal{C}\,\hat{\zeta} \end{aligned} \tag{17}$$

where $\hat{\zeta} = \left[\hat{i}_{\alpha s},\ \hat{i}_{\beta s},\ \hat{i}_{\alpha r},\ \hat{i}_{\beta r}\right]^T$ with $\hat{i}_{xx}$ as the estimated stator and rotor currents in $\alpha-\beta$, and $\mathrm{U} = [\,v_\alpha,\ v_\beta]^T$ (Fig. 2). The matrices associated with Luenberger observer are:

$$\mathcal{A}_{\mathcal{A}} = \begin{bmatrix} R_s\,L_r & -L_m^2\,w_r & -R_r\,L_m & -L_r\,L_m\,w_r \\ L_m^2\,w_r & R_s\,L_r & L_r\,L_m\,w_r & -R_r\,L_m \\ -R_s\,L_m & L_s\,L_m\,w_r & R_r\,L_s & L_r\,L_s\,w_r \\ -L_s\,L_m\,w_r & -R_s\,L_m & -L_r\,L_s\,w_r & R_r\,L_s \end{bmatrix}$$

$$\mathcal{A}(w_r) = \frac{1}{D1}\,\mathcal{A}_{\mathcal{A}}$$

$$\mathcal{B} = \frac{1}{D1}\begin{bmatrix} -L_r & 0 \\ 0 & -L_r \\ L_m & 0 \\ 0 & L_m \end{bmatrix} \qquad \mathcal{C} = \begin{bmatrix} 1 & 0 & 0 & 0 \\ 0 & 1 & 0 & 0 \end{bmatrix}$$

where $D1 = L_m^2 - L_s\,L_r$.

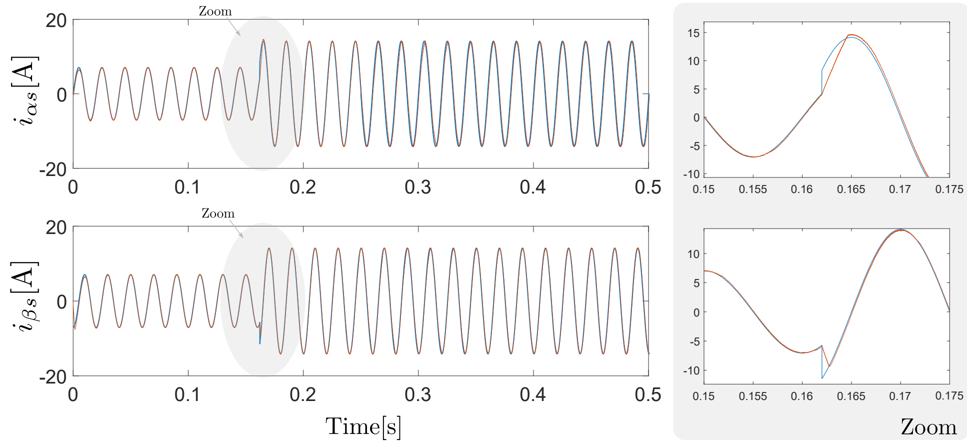

Fig. 3. Stator currents in $\alpha - \beta$ sub-space for transient and steady-state.

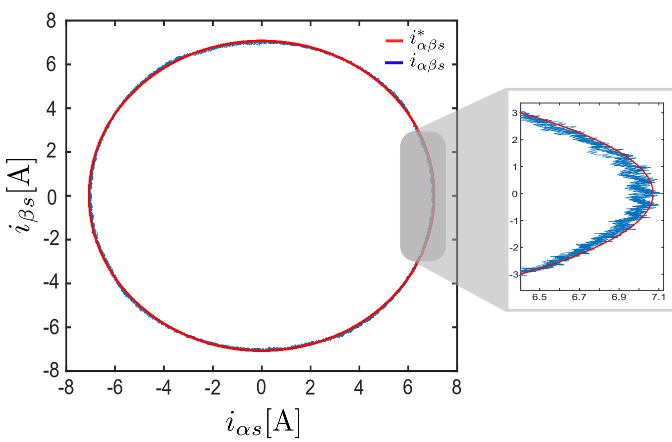

Fig. 4. Stator currents in the $\alpha - \beta$ planes for a desired AC currents ($i^*_{\alpha s}$, $i^*_{\beta s}$) of: 5[A] (RMS).

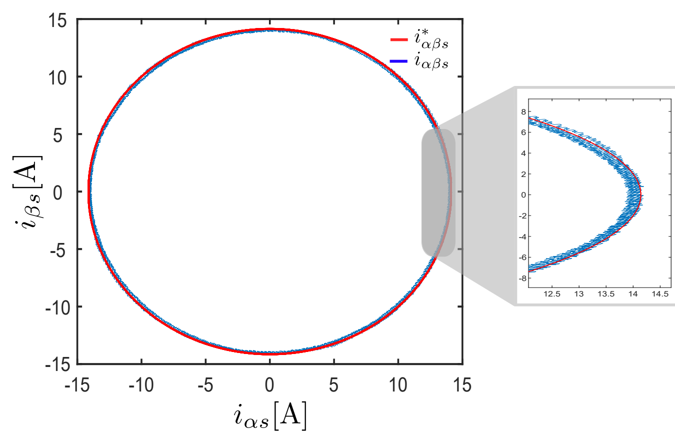

Fig. 5. Stator currents in the $\alpha - \beta$ planes for a desired AC currents ($i^*_{\alpha s}$, $i^*_{\beta s}$) of: 10 A (RMS).

IV. Theoretical Analysis by Simulations

By applying the equations that define the dynamics of the three-phase IM in simulations through MATLAB/Simulink software, the operation of the designed controller is evaluated. The mechanical and electrical parameters of the IM are shown in Table I.

TABLE I
PARAMETERS OF THREE-PHASE IM

R_s	0.7384 w	L_m	124.1 mH
R_r	0.7402 w	P	2
L_{ls}	3.045 mH	B	0.000503 kg.m^2/s
L_{lr}	3.045 mH	J	0.0343 kg.m^2
L_s	127.1 mH	Nominal speed	1500 rpm
L_r	127.1 mH	Nominal power	7.5 kW

Three-phase voltage source inverter (VSI) with V_{DC} = 620[V] and Sinusoidal Pulse Width Modulation (SPWM) with 15[kHz] switching frequency are used to power the IM.

The stator currents and mechanical speed of rotor are measured, and rotor currents are estimated using (17).

L matrix coefficients (18) and SMC's gains in Table II were found heuristically.

$$\mathrm{L} = \begin{bmatrix} 5726.60 & 0 \\ 0 & 5726.60 \\ -5712.55 & 0 \\ 0 & -5712.55 \end{bmatrix} \tag{18}$$

The simulation consists in the current control of a three-phase induction motor using the $\alpha - \beta$ reference frame (Fig. 3) with a constant load T_L = 1 N m, initially the desired AC currents ($i^*_{\alpha s}$, $i^*_{\beta s}$) have a RMS current value of 5 A, then at the instant 0.162 s with a step changes to an RMS current value of 10 A. As an uncertainty parameter, the mutual inductance L_m was varied, increasing its value to L_m = 170 mH, for the controller and the observer the L_m value is shown in the Table II and with this the results of Fig. 3, Fig. 4 and Fig. 5 were obtained.

TABLE II
SMC GAINS.

Gains	Values	Gains	Values
k_{11}	1000	K_i	100
k_{12}	1000	p	1
k_{21}	1000	a	20
k_{22}	1000	δ_0	0.01

V. Conclusions

In this work, a first-order sliding mode controller was simulated with exponential reaching law for three-phase motor induction, under uncertain conditions the controller performs well and can be improved by optimizing the controller's gains. The application of the proposed controller has been tested on simulations where the results obtained showed good reference tracking performance.

Acknowledgements

The authors would like to thank to the Paraguayan Government for the financial support through CONACYT by the Master in Electronic Engineering (POSG17-69). Also, we want to thank to Prof. Maarouf Saad for his teaching in nonlinear control in the Master's course in Paraguay.

References

[1] M. Kral and R. Gono, "Dynamic model of asynchronous machine," in *Proc. EPE*, pp. 1–4, May 2017.

[2] M. Ayala, J. Doval-Gandoy, J. Rodas, O. Gonzalez, and R. Gregor, "Current control designed with model based predictive control for six-phase motor drives," *ISA Transactions*, 2019.

[3] O. Gonzalez, M. Ayala, J. Rodas, R. Gregor, G. Rivas, and J. Doval-Gandoy, "Variable-speed control of a six-phase induction machine using predictive-fixed switching frequency current control techniques," in *Proc. PEDG*, pp. 1–6, June 2018.

[4] M. Ayala, J. Rodas, R. Gregor, J. Doval-Gandoy, O. Gonzalez, M. Saad, and M. Rivera, "Comparative study of predictive control strategies at fixed switching frequency for an asymmetrical six-phase induction motor drive," in *Proc. IEMDC*, pp. 1–8, Miami, FL, 2017.

[5] J. Rodas, C. Martin, M. R. Arahal, F. Barrero, and R. Gregor, "Influence of covariance-based ALS methods in the performance of predictive controllers with rotor current estimation," *IEEE Trans. Ind. Electron.*, vol. 64, no. 4, pp. 2602–2607, 2017.

[6] J. Rodas, F. Barrero, M. R. Arahal, C. Martin, and R. Gregor, "On-line estimation of rotor variables in predictive current controllers: A case study using five-phase induction machines," *IEEE Trans. Ind. Electron.*, vol. 63, no. 9, pp. 5348–5356, 2016.

[12] F. Wang, Z. Zhang, X. Mei, J. Rodríguez, and R. Kennel, "Advanced control strategies of induction machine: Field oriented control, direct torque control and model predictive control," *Energies*, vol. 11, no. 1, p. 120, 2018.

[7] J. Pedra, I. Candela, and L. Sainz, "Modelling of squirrel-cage induction motors for electromagnetic transient programs," *IET Electr. Power App.*, vol. 3, pp. 111–122, March 2009.

[8] S. D. Sudhoff, D. C. Aliprantis, B. T. Kuhn, and P. L. Chapman, "Experimental characterization procedure for use with an advanced induction machine model," *IEEE Trans. Energy Conv.*, vol. 18, pp. 48–56, March 2003.

[9] D. G. Taylor, "Nonlinear control of electric machines: an overview," *IEEE Control Systems Magazine*, vol. 14, pp. 41–51, Dec 1994.

[10] M. Hasoun, M. Khafallah, *et al.*, "Field oriented control of dual three-phase pmsm based vector space decomposition for electric ship propulsion," in *Proc. ICCSRE*, pp. 1–6, IEEE, 2019.

[11] A. G. Yepes, J. Malvar, A. Vidal, O. López, and J. Doval-Gandoy, "Current harmonics compensation based on multiresonant control in synchronous frames for symmetrical n-phase machines," *IEEE Trans. Ind. Electron.*, vol. 62, no. 5, pp. 2708–2720, 2014.

[13] X. Wang, Z. Wang, and Z. Xu, "A hybrid direct torque control scheme for dual three-phase pmsm drives with improved operation performance," *IEEE Trans. Power Electron.*, vol. 34, pp. 1622–1634, Feb 2019.

[14] Y. Kali, M. Saad, J. Doval-Gandoy, J. Rodas, and B. Khalid, "Discrete sliding mode control based on exponential reaching law and time delay estimation for an asymmetrical six-phase induction machine drive," *IET Electr. Power App.*, 09 2019.

[15] Y. Kali, M. Ayala, J. Rodas Bentez, M. Saad, J. Doval-Gandoy, R. Gregor, and K. Benjelloun, "Current control of a six-phase induction machine drive based on discrete-time sliding mode with time delay estimation," *Energies*, vol. 12, 01 2019.

[16] E. El-Gendy, A. F. Ibrahim, S. F. Saraya, and F. F. Areed, "A sliding mode controller for a three phase induction motor," *International Journal of Computer Applications*, vol. 64, no. 11, 2013.

[17] Y. Kali, M. Saad, and K. Benjelloun, *Control of Robot Manipulators Using Modified Backstepping Sliding Mode*, pp. 107–136. Singapore: Springer Singapore, 2019.

[18] C. Fallaha, M. Saad, and H. Kanaan, "Sliding mode control with exponential reaching law applied on a 3 dof modular robot arm," in *Proc. ECC*, pp. 4925–4931, July 2007.

[19] Y. Kali, J. Rodas, M. Saad, R. Gregor, K. Benjelloun, J. Doval-Gandoy, and G. Goodwin, "Speed control of a five-phase induction motor drive using modified super-twisting algorithm," in *Proc. SPEEDAM*, pp. 938–943, IEEE, 2018.

[20] C. J. Fallaha, M. Saad, H. Y. Kanaan, and K. Al-Haddad, "Sliding-mode robot control with exponential reaching law," *IEEE Trans. Ind. Electron.*, vol. 58, pp. 600–610, Feb 2011.

[21] R. Gregor and J. Rodas, "Speed sensorless control of dual three-phase induction machine based on a Luenberger observer for rotor current estimation," in *Proc. IECON*, pp. 3653–3658, Oct 2012.

[22] J. Rodas, R. Gregor, M. Rivera, Y. Takase, and M. Arzamendia, "Efficiency analysis of reduced-order observers applied to the predictive current control of asymmetrical dual three-phase induction machines," in *Proc. SLED/PRECEDE*, pp. 1–7, Oct 2013.

[23] R. Gregor, J. Rodas, D. Gregor, and F. Barrero, "Reduced-order observer analysis in MBPC techniques applied to the six-phase induction motor drives," in *Induction Motors*, ch. 13, Rijeka: IntechOpen, 2015.